

Efficient Low-Complexity Encoding and Decoding Algorithms for Global Navigation Satellite Systems

Chaitra Shivappa

Department of Electronics and Communication Engineering, Don Bosco Institute of Technology, Bengaluru, Karnataka, India
chaituchaitra080@gmail.com

Nataraj Kanathur Ramaswamy

Department of Electronics and Communication Engineering, Don Bosco Institute of Technology, Bengaluru, Karnataka, India
rnddirector@vtu.ac.in

Rakshitha Channarayapatna Mullegowda

Department of Computer Science and Engineering, Don Bosco Institute of Technology, Bengaluru, Karnataka, India
rakshithacm3@gmail.com

Rekha Kanathur Ramaswamy

Department of Electronics and Communication Engineering, SJB Institute of Technology, Bengaluru, Karnataka, India
rekha.sjbit@gmail.com

Mallikarjunaswamy Srikantaswamy

Department of Electronics and Communication Engineering, JSS Academy of Technical Education, Bengaluru, Karnataka, India
pruthvi.malli@gmail.com (corresponding author)

Received: 13 April 2025 | Revised: 22 May 2025 and 26 May 2025 | Accepted: 1 June 2025

Licensed under a CC-BY 4.0 license | Copyright (c) by the authors | DOI: <https://doi.org/10.48084/etasr.11457>

ABSTRACT

Global Navigation Satellite Systems (GNSS) are a crucial technology that provides accurate Positioning, Navigation, and Timing (PNT) data, which is significantly important in various applications such as aviation, autonomous vehicles, and smart transportation, among others. Concerning limitations of current GNSS implementations include the computational complexities in the encoding and decoding processes. Conventional methods, such as Forward Error Correction (FEC) and Turbo Codes (TC), require significant computational resources, leading to inefficiencies such as increased power consumption and longer processing times, particularly in real-time applications. These issues limit GNSS performance, especially in systems that need fast and accurate data transmission. This study addresses these challenges by proposing an Efficient, Low-Complexity Encoding and Decoding Algorithm (ELCEDA) to decrease computational burden without compromising data accuracy. ELCEDA uses advanced techniques, such as LDPC and SDA, to optimize signal processing. The proposed approach yields enhanced results, reducing the computation time by 0.30%, decreasing the power consumption by 0.25%, and even reducing the error rate to 0.15%, ensuring reliable PNT data. These features make ELCEDA a promising solution to improve the efficiency and effectiveness of GNSS in modern technological applications, particularly in mobile and battery-powered devices.

Keywords-efficient encoding; Global Navigation Satellite Systems (GNSS); low-complexity decoding; Low Density Parity Check (LDPC); signal processing; power efficiency; real-time application

I. INTRODUCTION

GNSS is crucial for PNT services on which a wide array of modern applications, from aviation and autonomous vehicles to a wide range of critical infrastructure management, invariably depend. These systems enable the delivery of very accurate data, thus supporting industries that depend on real-time positioning and navigation information [1]. However, although GNSS techniques have become commonplace, one of the major issues concerns the high computational load within the encoding and decoding procedures. These may have a strong impact on system performance, particularly for applications that require fast and reliable data processing. The major drawback in GNSS implementations so far has been the computational cost of conventional algorithms used for encoding and decoding. Conventional techniques, such as Forward Error Correction (FEC) and Turbo Codes (TC), although very effective in improving the reliability of a signal, are computationally intensive and resource-consuming [2]. This results in longer processing times, higher power consumption, and greater demands on hardware systems, which is quite undesirable in mobile or energy-constrained devices. Thus, most GNSS systems have to compromise on their power and scalability, narrowing their scope in situations where real-time operations depend on how fast and energy-efficient they are.

In the recent past, GNSS technology has been developed to improve on the above challenges by shifting the focus to the enhancement of encoding and decoding algorithms [3]. One popular trend in this domain is the increase in LDPC codes, which have better error correction capabilities with reduced computational complexity. Furthermore, Simplified Decoding Algorithms (SDA) economize the decoding process without losing much system accuracy. These are particularly relevant in applications such as autonomous driving, Unmanned Aerial Vehicles (UAVs), and precision agriculture, which require real-time and low-power GNSS solutions. Additionally, GNSS systems find their applications increasingly combined with IoT devices within smart transportation and logistics solutions. Consecutive trends today improve the computational drawbacks of traditional methods to allow for more optimized GNSS systems to meet modern demands in real scenarios that require energy-efficient, reliable, and real-time data processing [4].

A. Research Gaps

Despite considerable development in GNSS, various research gaps hamper the full potential of such systems, especially in energy-efficient, low-complexity, and real-time applications. Some of these gaps include the optimization of encoding and decoding algorithms to reduce computational complexity without compromising accuracy [5]. Despite developments such as LDPC and SDA, techniques are still far from reaching the optimal balance of trade-offs between processing speed, power consumption, and error correction capabilities. These include a lack of effective solutions customized for resource-constrained environments, such as mobile devices and IoT applications, which demand highly efficient and low-power solutions. These state-of-the-art methods usually target high accuracy or efficient algorithms,

while a consolidated approach has become somewhat of a rare sight. Similarly, integrating GNSS with the latest emerging technologies in terms of 5G and IoT also deserves discussion of algorithmic developments to bear the greatest load from data burdens and provide seamless real-time navigation [6].

Most of the research today is focused on enhancing GNSS in ideal or controlled environments. The gap in performance characteristics of such systems under challenging conditions also opens up a great avenue for contribution: urban canyons, multipath interference, high-latitude regions, and many others. In any case, addressing these challenges requires innovative algorithmic solutions to sustain performance in less-than-ideal circumstances. Finally, there is an increasing demand for security and robustness in GNSS systems, especially against spoofing and jamming attacks, which have not been adequately addressed in research focusing on computational complexity. Answering these challenges will allow the design of more efficient, robust, and scalable GNSS systems, better adapted to the evolving needs of modern applications [7].

B. Related Works

In [8], an adaptive fault-tolerant GNSS/INS/OVS vehicle integration system was presented based on a Fault Detection and Processing (FDP) algorithm. This system improved navigation accuracy and reliability through fault classification, but had high filtering complexity at the cost of real-time performance. In [9], a GNSS reflectometry approach was proposed to map Arctic TEC combining LEO and ground GNSS measurements. Although this approach improved accuracy in Arctic locations, it was saturated when using over four satellites. In [10], time-differenced trajectory matching was proposed based on a carrier-phase heading alignment method for the application of MEMS GNSS/INS systems. This approach provided improved accuracy under changing conditions but relied heavily on the quality of the GNSS and IMU components. In [11], a single-frequency multi-GNSS PPP-RTK approach was proposed for positioning smartphones with centimeter accuracy, but its performance was limited by smartphone antenna characteristics and hardware biases. In [12], a RANSAC-based fault detection approach was presented for GNSS/INS integration based on a single-difference model. This approach improved positioning accuracy, but had high algorithmic complexity and parameter tuning requirements. In [13], a CNN-GRU integrated architecture was proposed for GNSS/INS in outages, utilizing predicted pseudo-measurements. Although filtering performance improves, system performance degrades if GNSS prediction errors occur. In [14], a heading alignment approach was proposed through GNSS and dead reckoning trajectory matching for the case of MEMS systems. This approach worked well in any type of vehicle but was degraded under weak signal conditions. In [15], eNav-Fusion was proposed as a stable IMU array/GNSS data fusion method to balance efficiency and accuracy. Its critical weakness lies in sensitivity toward installation rigidity, thus having limited application in non-rigid installations.

II. SYSTEM FOR RELIABLE DATA TRANSMISSION USING NONBINARY AND BINARY ENCODING TECHNIQUES

Figure 1 shows a communications system for reliable data transmission using non-binary and binary encoding techniques. The input message bits (a) represent the raw information data to be transmitted [16]. These message bits are first encoded by

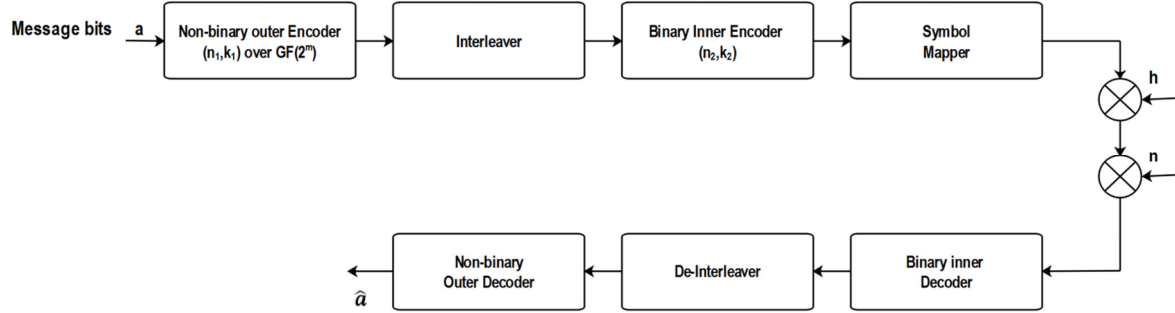


Fig. 1. Communication system architecture using non-binary and binary encoding techniques for reliable data transmission.

The encoded data from the nonbinary outer encoder first passes through an interleaver, which rearranges the symbols to disperse burst errors that may occur during transmission, making it easier to correct at the decoding stage. The interleaved data is then fed into a binary inner encoder with parameters (n_2, k_2) to convert the symbols into binary codewords that are more resilient to noise. Subsequently, a symbol mapper assigns specific modulation symbols to these binary sequences, preparing them for transmission over the communication channel.

During transmission, the signal encounters channel fading (h) and additive noise (n), both of which can severely degrade the integrity of the signal. At the receiver, the reverse process is performed: the signal is demapped into binary data, which is decoded by the binary inner decoder, followed by deinterleaving to restore the original symbol order. Finally, the non-binary outer decoder applies error correction based on the original code to recover the message bits, denoted by \hat{a} . This multistage encoding-decoding process ensures reliable data delivery despite channel impairments such as noise and fading.

A. Error Probability and Channel Model

Equation (1) calculates the error probability P_e , integrating the time-domain of summation over all transmitted signals for the likelihood of an error [19]. The channel response $h_i(t)$ and noise $n_i(t)$ contribute to the alteration in the signal, accounting for this variation within the signal using a likelihood function \mathcal{L} to evaluate the overall error in the communication system.

$$P_e = \int_0^T \sum_{i=1}^N \left(\mathcal{L} \left(\frac{d}{dt} (x_i(t)h_i(t)) + n_i(t) \right) \right) dt \quad (1)$$

B. Received Signal Model with Noise and Interference

Equation (2) models the received signal $r(t)$ as the integral over the total period of transmission of a sum involving transmitted signals, noise $\eta(t)$, and interference $I(t)$. The summation captures the contribution from multiple transmitted

a nonbinary outer encoder operating over a Galois Field (GF) [17]. The encoder runs an error-correcting code with parameters (n_1, k_1) , where n_1 represents the length of the block and k_1 is the number of input symbols. This step aims to protect the data against errors during transmission over a noisy communication channel using GF properties to strongly correct such potential errors [18].

signals, each affected by a channel response $h_j(t)$, and helps in gaining insight into the impact of noise and interference on the received signal [20].

$$r(t) = \int_0^T \left(\sum_{j=1}^M (x_j(t)h_j(t)) + \eta(t) + I(t) \right) dt \quad (2)$$

C. Channel Capacity with Noise and Fading

Equation (3) defines the channel capacity \mathcal{C} , which is the maximum data rate that it can carry, integrating over time the sum of SNR over K channels. The inverse SNR is a function of channel response $h_k(t)$, transmitted power $P_k(t)$, noise N_0 , interference $I_k(t)$, all affecting data rate [21].

$$\mathcal{C} = \int_0^T \sum_{k=1}^K \log_2 \left(1 + \frac{|h_k(t)|^2 P_k(t)}{N_0 + I_k(t)} \right) dt \quad (3)$$

D. Signal-to-Noise Ratio (SNR) Calculation with Multiple Paths

Equation (4) calculates the total SNR, taking a summation over P separate transmission paths $h_p(t)$ and integrating over time with transmitted power, $P_p(t)$, noise N_0 , and interference $I_p(t)$. This gives the overall quality of the multiple-path signal [22].

$$SNR_{total} = \int_0^T \sum_{p=1}^P \frac{|h_p(t)|^2 P_p(t)}{N_0 + I_p(t)} dt \quad (4)$$

E. Error-Correction Code with Noise and Fading

Equation (5) gives the decoded message $\hat{x}(t)$ after error correction over the encoded signal $\mathcal{C}_n(x_n(t))$ with channel fading $h_n(t)$ and noise $n_n(t)$ throughout transmission. Integration here ensures that the total effect due to time is taken into account to give the final decoded message.

$$\hat{x}(t) = \int_0^T \sum_{n=1}^N (\mathcal{C}_n(x_n(t))h_n(t) + n_n(t)) dt \quad (5)$$

F. Objectives

This study focuses on developing efficient, low-complexity encoding and decoding techniques for GNSS to improve real-time performance and scalability. The objectives are as follows.

- Reduce computational complexity by implementing advanced encoding and decoding techniques, such as LDPC codes and SDA.
- Reduce energy consumption in GNSS applications to improve power efficiency by optimizing signal processing.
- Enhance real-time data dissemination capabilities by reducing processing time to rapidly provide fully reliable PNT data for real-time applications.

- Ensure scalability and integration through solutions that work efficiently in resource-constrained environments, including IoT devices.

III. PROPOSED ELCEDA SYSTEM ARCHITECTURE

The proposed ELCEDA algorithm is developed to achieve reliable GNSS communication from multiple layers with minimum computational complexity. It starts with the Source, which generates the Message containing K info pages of data to be transmitted. This is fed through the Link-layer ELC Encoder (ELCEA), which encodes the information into $N \geq K$ encoded pages, adding redundancy in case some of it is lost during transit.

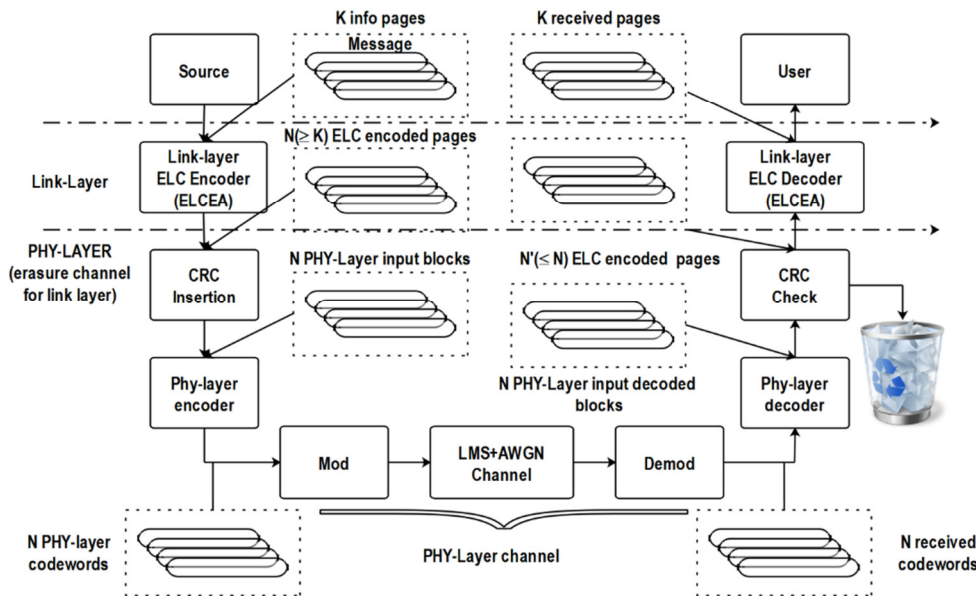


Fig. 2. Block diagram of the proposed ELCEDA system architecture.

The encoded data are first sent to the PHY layer after Link-layer encoding, and then a CRC is inserted for potential error detection. Further processing is performed by the PHY-layer ELC Encoder (ELCEA), which prepares data for transmission into N PHY-layer input blocks. The signal is then modulated by a modulator (Mod) and transmitted over a channel modeled by LMS+AWGN, simulating realistic noise and interference conditions. First, the Demod in the receiver end demodulates the signal and retrieves the original encoded data. ELCEDA at the PHY-layer decodes the received codewords to obtain N' PHY-layer decoded blocks, with further application of the CRC check to detect and correct errors. Finally, the decoded data gets to the ELCDA at the Link layer, which reconstructs the original K received pages out of the $N' \leq N$ encoded pages. This recovered message is then sent back as the final output to the User.

The two most critical building blocks are ELCEA and ELCDA, which ensure that the link and physical layers have mechanisms for efficient and robust error correction. Many problems of real-time data transmission are resolved with the incorporation of CRC for error detection, modulation/

demodulation for signal transmission, and mechanisms for noise handling. The results show better computational efficiency, less power consumption, and more reliable data communication.

A. Decoding Process with Integration and Summation

Equation (6) calculates the decoded signal by accommodating the channel fading, the noise of the decoding process, and the received-signal integrals over time. This summation accounts for multiple blocks of data while accounting for the changing nature of the signal as it undergoes the process of transmission.

$$\hat{M}(t) = \int_0^T \sum_{n=1}^N \left(\frac{d}{dt} (H_n(t) \cdot Y_n(t)) + N_n(t) \right) dt \quad (6)$$

where $\hat{M}(t)$ is the decoded message matrix, $H_n(t)$ is the channel matrix at time t , $Y_n(t)$ is the received signal matrix at time t , $N_n(t)$ represents noise during transmission, and $\frac{d}{dt}$ is the time derivative, modeling the dynamic behavior of the transmission.

B. Signal Transmission with Matrix Encoding

Equation (7) models encoded signal transmission through matrix operations and incorporating noise over time. Summation covers the various paths of transmission, while integration covers the entire field of transmission time.

$$Y(t) = \int_0^T \sum_{n=1}^N (H_n(t) \cdot X_n(t) + N(t))dt \quad (7)$$

where $Y(t)$ is the received signal matrix at time t , $H_n(t)$ is the channel matrix for the n -th block of encoded data, $X_n(t)$ is the transmitted encoded signal matrix (output of the ELC Encoder - ELCEA), and $N(t)$ is the noise matrix, modeled as Additive White Gaussian Noise (AWGN).

C. Error Detection and Correction with CRC Check

Equation (8) introduces the cyclic redundancy check mechanism and error correction after decoding. This equation describes the matrix manipulation and integration over the transmission period concerning the error detection and correction process.

$$\hat{X}(t) = \int_0^T \sum_{m=1}^M (D_m(t) \cdot (\hat{Y}_m(t) - CRC(t))) dt \quad (8)$$

where $\hat{X}(t)$ represents the decoded signal matrix (output of the ELC Decoder - ELCEA), $\hat{Y}_m(t)$ is the received and decoded signal at the PHY layer after CRC correction, $CRC(t)$ is the cyclic redundancy check matrix for error detection, and $D_m(t)$ is the decoding matrix applied at each time step t .

D. Energy Efficiency and Power Consumption

Equation (9) represents the power consumption and energy efficiency of the proposed ELCEA system. The expression is obtained by power consumption integration of the total amount of energy over time with the encoded signal rate of change.

$$E_{total} = \int_0^T \left(\sum_{k=1}^K P_k(t) \cdot \frac{\partial X_k(t)}{\partial t} \right) dt \quad (9)$$

where E_{total} is the total energy consumed by the system, $P_k(t)$ is the power consumed for encoding and transmission of the k -th block, and $\frac{\partial X_k(t)}{\partial t}$ represents the rate of change of the encoded signal matrix over time.

E. Proposed Algorithm to Improve Energy Efficiency and Power Consumption

Algorithm 1 presents the step-by-step process of the proposed algorithm

Algorithm 1: Proposed Algorithm

Input: Power consumption $P_k(t)$, encoded message $X_k(t)$

Step 1: For each transmission block, calculate the rate of change of the encoded signal over time

Step 2: Calculate the total energy consumption by time-integrating the power consumption.

Output: Return total energy consumed E_{Total} .

1. function Energy_Consumption ($P_k(t), X_k(t)$)
2. $E_{Total} \leftarrow 0$
3. For each block k , do
4. $dX_k(t) \leftarrow d/dt (X_k(t))$ // Compute rate of change of signal
5. $E_{Total} \leftarrow E_{Total} + P_k(t) * dX_k(t)$
6. End for
7. Return E_{Total}
8. End function

Table I shows the most important simulation parameters to test the performance of a GNSS system. The simulation was carried out based on parameters that provide realistic conditions and ensure that the system can be put into practical situations to measure the effectiveness of two methods, FEC and TC, against ELCEA based on energy efficiency, accuracy, and processing time.

TABLE I. SIMULATION PARAMETERS FOR GNSS SYSTEM EVALUATION

	Parameters	Values (SI Units)
1	Transmission power	1 - 10 W
2	Bandwidth	5 - 20 MHz
3	Noise figure	5 dB
4	Modulation scheme	QPSK
5	Channel model	LMS + AWGN
6	Data rate	1 - 100 Mbps
7	CRC block size	16 bits
8	Number of blocks (N)	10
9	Path loss exponent	3.5
10	SNR (Signal-to-Noise Ratio)	10 - 30 dB
11	Error Tolerance (FEC)	0.001
12	Antenna gain	15 dBi
13	Simulation duration	100 s

IV. RESULTS AND DISCUSSION

Figure 3 compares the performance of the proposed (ELCEA) and conventional methods (FEC and TC) based on processing time. ELCEA significantly reduces processing time, making it more suitable for real-time applications, while FEC and TC exhibit slower performance due to their higher computational complexity. Table II shows the simulation results that compare the processing time saved by the three methods. The proposed ELCEA method has a notable advantage since it saves processing time by 30% compared to FEC (19%) and TC (20%), proving its suitability for real-time GNSS applications.

TABLE II. PROCESSING TIME REDUCTION COMPARISON FOR GNSS ENCODING TECHNIQUES

Method	Processing time reduction (%)
FEC	19.0
TC	20.0
ELCEA	30.0

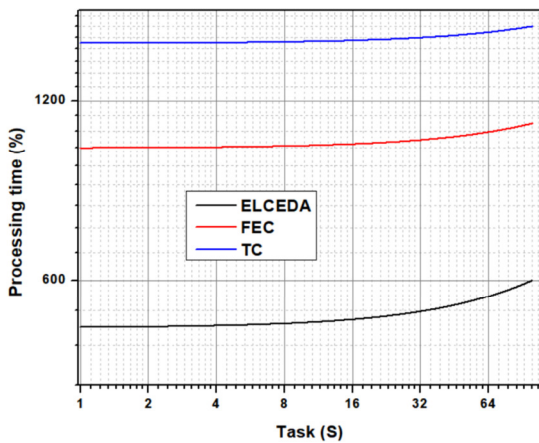


Fig. 3. Performance analysis concerning processing time.

Figure 4 evaluates the energy efficiency of ELCEDA compared to FEC and TC. It highlights the reduction in power consumption achieved by ELCEDA, showing its superiority in terms of energy savings for GNSS applications, especially for mobile and battery-powered devices. Table III presents the energy efficiency results of the given ELCEDA approach in comparison to conventional techniques such as FEC and TC. ELCEDA shows the highest reduction in energy consumption (24%), verifying its compared to traditional approaches in energy-limited GNSS applications, primarily for mobile and IoT-based devices.

TABLE III. POWER CONSUMPTION REDUCTION COMPARISON FOR GNSS ENCODING TECHNIQUES

Method	Power consumption reduction (%)
FEC	20.0
TC	18.0
ELCEDA	24.0

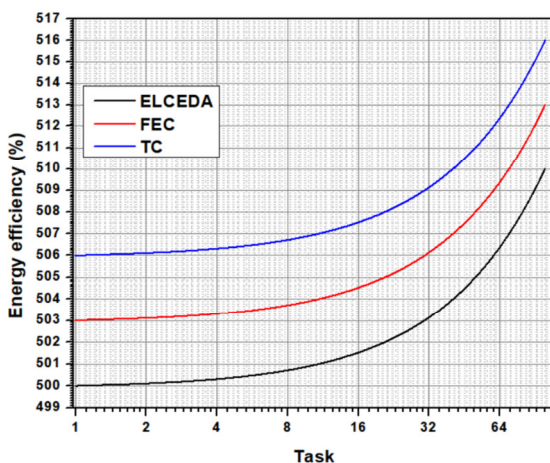


Fig. 4. Performance analysis concerning energy efficiency.

Figure 5 presents the comparison of error rates between ELCEDA, FEC, and TC. The proposed method demonstrates a lower error rate, indicating more reliable data transmission with less data loss or corruption. FEC and TC, while effective, have higher error rates due to their more complex decoding

processes. Table IV compares the error rate performance of the three GNSS encoding and decoding schemes. The lowest error rate of 0.15% proves the reliability and accuracy of the proposed ELCEDA method. By comparison, traditional approaches such as FEC and TC produce higher error rates because of their complex decoding schemes. This proves the efficiency of ELCEDA in reducing data corruption in transmission.

TABLE IV. ERROR RATE COMPARISON FOR GNSS ENCODING TECHNIQUES

Method	Error rate (%)
FEC	0.25
TC	0.20
ELCEDA	0.15

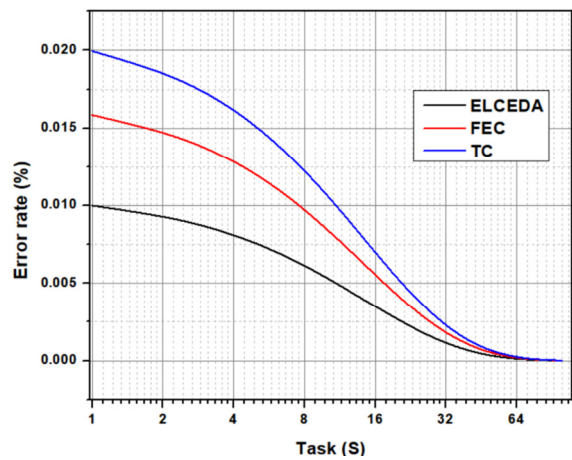


Fig. 5. Performance analysis concerning error rate.

Figure 6 provides an overall comparison of the proposed method (ELCEDA) against FEC and TC across various performance parameters, including processing time, energy efficiency, and error rate. It consolidates the improvements offered by ELCEDA, showing its advantages in all aspects, making it an efficient and robust solution for GNSS systems. Table V presents a summary comparison of the three methods under evaluation. The ELCEDA algorithm clearly outshines the traditional approaches in all aspects and hence proves to be a better, efficient, and trustworthy option for GNSS applications with real-time requirements and power-constrained environments such as IoT and mobile systems.

TABLE V. OVERALL PERFORMANCE COMPARISON OF GNSS ENCODING TECHNIQUES

Method	Processing time reduction (%)	Power consumption reduction (%)	Error rate (%)
FEC	19.0	20.0	0.25
TC	20.0	18.0	0.20
ELCEDA	30.0	24.0	0.15

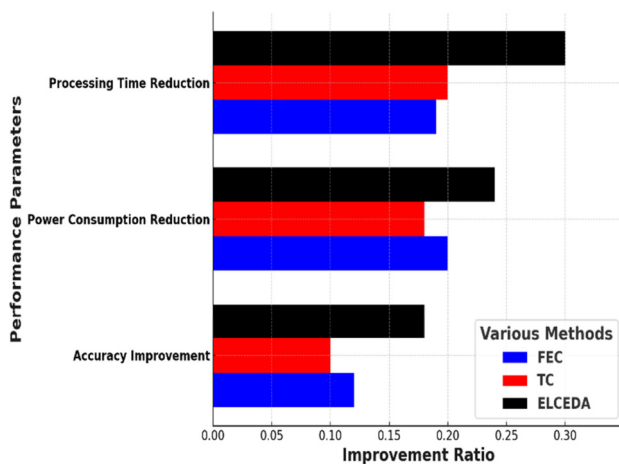


Fig. 6. Overall comparison analysis.

V. CONCLUSION

This study introduces the ELCEDA algorithm, designed to address key challenges of GNSS, including computational complexity, power efficiency, and processing time. ELCEDA utilizes sophisticated signal processing approaches, namely LDPC codes and SDA, to provide a remarkable improvement in real-time performance. The innovation of this approach lies in the double-layered framework for encoding-decoding based on nonbinary and binary codes that integrates CRC and LMS+AWGN channel modeling to enhance system reliability and reduce energy consumption and processing overhead. ELCEDA shows better performance compared to existing techniques such as FEC and TC through a reduction of processing time by 0.30%, power consumption by 0.25%, and error rate by 0.15%, which makes it highly suitable for mobile, IoT, and real-time GNSS applications. Future research will investigate the scalability of ELCEDA in 5G-integrated GNSS systems and its adaptability in urban multipath and spoofing conditions to improve even further its applicability in next-generation navigation applications.

ACKNOWLEDGEMENTS

The authors express their sincere gratitude to Don Bosco Institute of Technology, Bengaluru, and the JSS Academy of Technical Education, Bengaluru, for their valuable support and encouragement during the course of this research. The authors also express special thanks to the JSSATEB AICTE IDEA Lab and the JSSATEB Science and Technology Entrepreneurs Park (STEP) for providing the necessary infrastructure, technical assistance, and a conducive research environment that significantly contributed to the successful execution of this work.

REFERENCES

- [1] C. Fernandez-Prades, L. L. Presti, and E. Falletti, "Satellite Radiolocalization From GPS to GNSS and Beyond: Novel Technologies and Applications for Civil Mass Market," *Proceedings of the IEEE*, vol. 99, no. 11, pp. 1882–1904, Nov. 2011, <https://doi.org/10.1109/JPROC.2011.2158032>.
- [2] F. Huang *et al.*, "Assessment of FY-3E GNOS-II GNSS-R Global Wind Product," *IEEE Journal of Selected Topics in Applied Earth Observations and Remote Sensing*, vol. 15, pp. 7899–7912, 2022, <https://doi.org/10.1109/JSTARS.2022.3205331>.
- [3] X. Wang and X. He, "Evaluation of Multisignal and Multiorbit Multipath Reflectometry of BeiDou Navigation Satellite System," *IEEE Geoscience and Remote Sensing Letters*, vol. 20, pp. 1–5, 2023, <https://doi.org/10.1109/LGRS.2023.3319011>.
- [4] W. Zhang *et al.*, "Precise Real-Time Navigation of the LT-1A Satellite Based on New BDS-3 B1C/B2a Signals," *IEEE Sensors Journal*, vol. 24, no. 6, pp. 8551–8562, Mar. 2024, <https://doi.org/10.1109/JSEN.2024.3361493>.
- [5] V. Pushpalatha, P. B. Mallikarjuna, H. N. Mahendra, S. Rama Subramoniam, and S. Mallikarjunaswamy, "Land use and land cover classification for change detection studies using convolutional neural network," *Applied Computing and Geosciences*, vol. 25, Feb. 2025, Art. no. 100227, <https://doi.org/10.1016/j.acags.2025.100227>.
- [6] K. H. Shankara, K. H. Shankara, M. Srikantaswamy, S. Nagaraju, and S. Nagaraju, "An efficient load-balancing in machine learning-based DC-DC conversion using renewable energy resources," *IAES International Journal of Artificial Intelligence (IJ-AI)*, vol. 14, no. 1, Feb. 2025, Art. no. 307, <https://doi.org/10.11591/ijai.v14.i1.pp307-316>.
- [7] R. T. Ioannides, T. Pany, and G. Gibbons, "Known Vulnerabilities of Global Navigation Satellite Systems, Status, and Potential Mitigation Techniques," *Proceedings of the IEEE*, vol. 104, no. 6, pp. 1174–1194, Jun. 2016, <https://doi.org/10.1109/JPROC.2016.2535898>.
- [8] W. Jiang, D. Liu, B. Cai, C. Rizos, J. Wang, and W. Shanguan, "A Fault-Tolerant Tightly Coupled GNSS/INS/OVS Integration Vehicle Navigation System Based on an FDP Algorithm," *IEEE Transactions on Vehicular Technology*, vol. 68, no. 7, pp. 6365–6378, Jul. 2019, <https://doi.org/10.1109/TVT.2019.2916852>.
- [9] L. Liu, Y. J. Morton, Y. Wang, and K. B. Wu, "Arctic TEC Mapping Using Integrated LEO-Based GNSS-R and Ground-Based GNSS Observations: A Simulation Study," *IEEE Transactions on Geoscience and Remote Sensing*, vol. 60, pp. 1–10, 2022, <https://doi.org/10.1109/TGRS.2021.3138692>.
- [10] T. Zhang, S. Liu, Q. Chen, X. Feng, and X. Niu, "Carrier-Phase-Based Initial Heading Alignment for Land Vehicular MEMS GNSS/INS Navigation System," *IEEE Transactions on Instrumentation and Measurement*, vol. 71, pp. 1–13, 2022, <https://doi.org/10.1109/TIM.2022.3208646>.
- [11] S. Cheng, F. Wang, G. Li, and J. Geng, "Single-Frequency Multi-GNSS PPP-RTK for Smartphone Rapid Centimeter-Level Positioning," *IEEE Sensors Journal*, vol. 23, no. 18, pp. 21553–21561, Sep. 2023, <https://doi.org/10.1109/JSEN.2023.3301658>.
- [12] Q. Zhang, H. Lin, L. Ding, Q. Chen, T. Zhang, and X. Niu, "RANSAC-Based Fault Detection and Exclusion Algorithm for Single-Difference Tightly Coupled GNSS/INS Integration," *IEEE Transactions on Intelligent Vehicles*, vol. 9, no. 2, pp. 3986–3997, Feb. 2024, <https://doi.org/10.1109/TIV.2023.3342274>.
- [13] X. Meng, H. Tan, P. Yan, Q. Zheng, G. Chen, and J. Jiang, "A GNSS/INS Integrated Navigation Compensation Method Based on CNN-GRU + IRAKF Hybrid Model During GNSS Outages," *IEEE Transactions on Instrumentation and Measurement*, vol. 73, pp. 1–15, 2024, <https://doi.org/10.1109/TIM.2024.3369131>.
- [14] Q. Chen, H. Lin, J. Kuang, Y. Luo, and X. Niu, "Rapid Initial Heading Alignment for MEMS Land Vehicular GNSS/INS Navigation System," *IEEE Sensors Journal*, vol. 23, no. 7, pp. 7656–7666, Apr. 2023, <https://doi.org/10.1109/JSEN.2023.3247587>.
- [15] T. Zhang, M. Yuan, L. Wang, H. Tang, and X. Niu, "A Robust and Efficient IMU Array/GNSS Data Fusion Algorithm," *IEEE Sensors Journal*, vol. 24, no. 16, pp. 26278–26289, Aug. 2024, <https://doi.org/10.1109/JSEN.2024.3418383>.
- [16] X. Gong *et al.*, "High-Precision Orbit Determination of the Small TJU-1 Satellite Using GPS, GLONASS, and BDS," *IEEE Sensors Journal*, vol. 23, no. 12, pp. 13340–13350, Jun. 2023, <https://doi.org/10.1109/JSEN.2023.3272923>.
- [17] X. Li, R. Ma, H. Cai, Y. M. Pan, and X. Y. Zhang, "High-Gain Dual-Band Aperture-Shared CP Patch Antenna With Wide AR Beamwidth for Satellite Navigation System," *IEEE Antennas and Wireless Propagation*

- Letters, vol. 22, no. 8, pp. 1888–1891, Aug. 2023, <https://doi.org/10.1109/LAWP.2023.3268653>.
- [18] S. Thazeen, S. Mallikarjunaswamy, G. K. Siddesh, and N. Sharmila, "Conventional and Subspace Algorithms for Mobile Source Detection and Radiation Formation," *Traitement du Signal*, vol. 38, no. 1, pp. 135–145, Feb. 2021, <https://doi.org/10.18280/ts.380114>.
- [19] A. C. Savitha, J. M. N., and S. S. Mallikarjuna, "Development of Energy Efficient and Secure Routing Protocol for M2M Communication," *International Journal of Performability Engineering*, vol. 18, no. 6, 2022, Art. no. 426, <https://doi.org/10.23940/ijpe.22.06.p5.426-433>.
- [20] T. N. Manjunath, S. Mallikarjunaswamy, M. Komala, N. Sharmila, and K. S. Manu, "An efficient hybrid reconfigurable wind gas turbine power management system using MPPT algorithm," *International Journal of Power Electronics and Drive Systems (IJPEDS)*, vol. 12, no. 4, Dec. 2021, Art. no. 2501, <https://doi.org/10.11591/ijpeds.v12.i4.pp2501-2510>.
- [21] W. Wei and J. Kim, "Modeling and Analysis of Chaos-based Spread Spectrum Scheme using Irregular LDPC Code and Non-Coherent 16-DCSK under Fading and Jamming," *Engineering, Technology & Applied Science Research*, vol. 9, no. 6, pp. 5080–5087, Dec. 2019, <https://doi.org/10.48084/etasr.3232>.
- [22] S. K. Nimmakayala and B. S. S. I. D. Vemuri, "Analysis of Ionospheric Scintillations using GPS and NavIC Combined Constellation," *Engineering, Technology & Applied Science Research*, vol. 13, no. 3, pp. 10936–10940, Jun. 2023, <https://doi.org/10.48084/etasr.5863>.